MEASURING SNOW PRESSURE FORCES ON SUPPORTING STRUCTURES USING LOW-COST STRAIN GAUGES

Joël Borner[1,2,*], Patrik Rusterholz[3], Stefan Margreth[1], Perry Bartelt[1,2]

[1] *WSL Institute for Snow and Avalanche Research SLF, Davos, Switzerland*
[2] *Climate Change, Extremes and Natural Hazards in Alpine Regions Research Centre CERC, Davos, Switzerland*
[3] *FERUGEN GmbH, Bubikon, Switzerland*

ABSTRACT: Predicting snow pressure forces exerted by the snow cover on structures on sloping terrain remains a challenging task. Especially with the increasing interest in alpine solar parks with little financial margin for safety, the demand for monitoring systems as well as accurate prediction models for snow pressure acting on slender supports is higher than ever before. This paper presents an experimental setup for measuring the reaction forces of the snow cover on various support and pressure bars of an snow supporting structure made of steel using strain gauges. In combination with the material properties and the entire static system of the structure, we can back calculate the pressure exerted by the snow cover. In order to interpret the measured forces correctly, additional field campaigns in winter are important to determine the local snow distribution, the snow temperature and the density of the snow cover. We extensively address challenges encountered during the measurement campaign, including eliminating temperature-induced strain, amplifying the signal in low strain ranges, handling combined bending and restraint stresses, and protecting sensors and cables against settlement and creep forces. Having overcome these challenges, the key advantages of using strain gauges are that the system is cost effective and non-invasive and therefore allows rapid installation on a large number of sections of interest. We discuss results obtained from the first winter of the campaign (2023/2024). The high measurement frequency of one measurement every five minutes provides an insight into the daily cycle of the forces. Most notably, on warm spring days with cold nights, we observed a continuous increase in forces starting at sunset, peaking at sunrise, followed by a rapid decline thereafter. The measurement data can be used to calibrate newly developed viscoelastic 3D snow creep models with various constitutive laws for the prediction of creep and glide forces on supporting structures. These models as well as the presented experimental setup show great potential to further optimise the design of supporting structures and installations of alpine solar parks.

Keywords: strain gauges, snow pressure monitoring, supporting structures

1. INTRODUCTION

Snow-supporting structures are one of the most important and commonly used active measures for avalanche control (Margreth et al., 2014). They help mitigate avalanche hazards by decreasing both the likelihood and the potential size of avalanches. During the avalanche winter of 1999, these measures proved highly effective; one assessment estimated that snow-supporting structures in Switzerland successfully prevented 300 destructive avalanches (SLF, 2000).
While research in the past years mainly focused on new numeric models (see Podolskiy et al. (2013)), practitioners and guidelines (Margreth, 2007) still rely on simple analytical models (e.g., Bader et al. (1939), Haefeli (1939), Salm (1977)) when it comes to the static design of supporting structures. The main reason for this is that analytical solutions are more intuitive than numerical solutions for understanding the dependencies of snow pressure on easy-to-measure input parameters such as slope inclination, snow depth and snow density (Fellin, 2013).

In addition, the availability of measurement data is still scarce. Hiller and Bader (1990) measured the snow pressure on supporting structures at six locations in Switzerland over a period of 20 years using a load measuring device mounted on the girder of the instrumented steel bridge. Larsen et al. (1985) instrumented masts over a period of 25 years using vibrating wires as strain gauges. This paper presents an experimental setup to measure snow pressure on steel structures using low-cost Wheatstone bridges in combination with the static system of the structure. The first winter of the measurement campaign (2023/2024) showed some promising results, but also some questionable force values. The causes of these drawbacks are discussed in this paper and countermeasures are already being taken to improve the system for the next winter of the campaign.

*Corresponding author address:
Joël Borner, WSL Institute of Snow and Avalanche Research SLF
7260 Davos Dorf, Switzerland;
tel: ++41 814170866
email: joel.borner@slf.ch

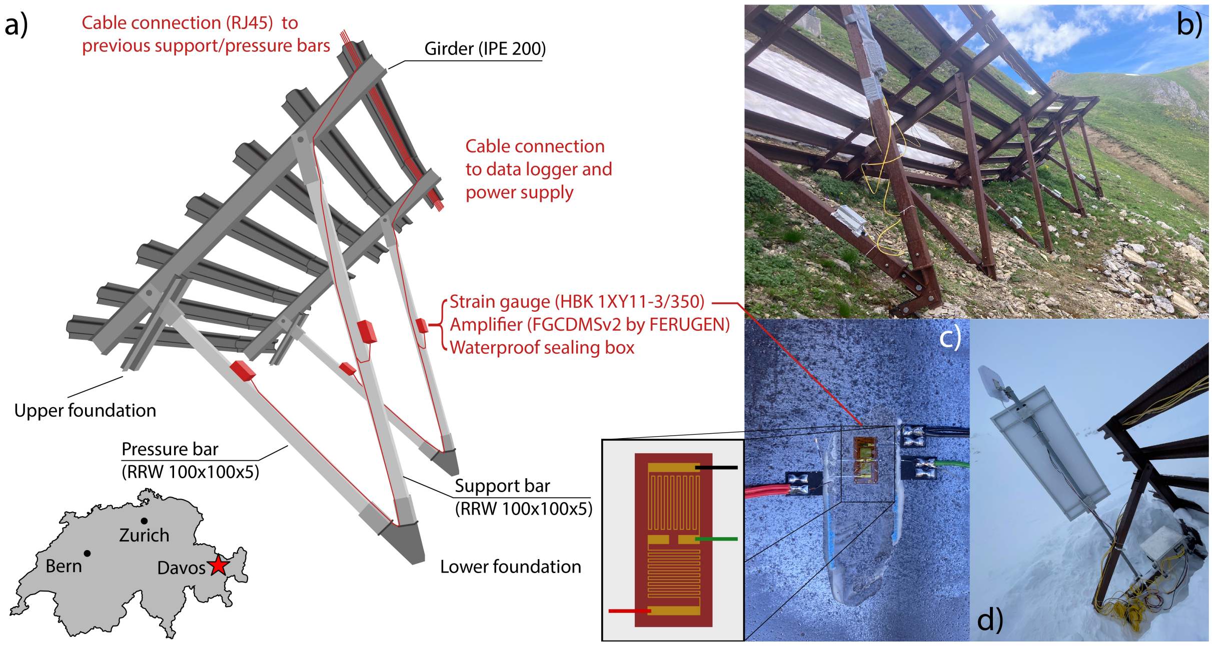

Figure 1: Experimental setup of the supporting structure: a) schematic overview of one field of the supporting structure with all measurement points as well as cable connections. b) Measurement points of the northernmost four fields on support and pressure bars. c) Strain gauge with two measuring grids for temperature correction. d) Box with data logger, main board, battery and router. Solar panel with antenna for real-time data transmission.

2. INSTRUMENTAL SETUP

The instrumented supporting structure "Seetälli" (46.853567° N; 9.816216° E) is located in the Davos Parsenn ski area in Switzerland at an altitude of 2403 m.a.s.l. It is the lower of two rows, which are approximately 25 m apart. The slope is 30-35° steep and faces east. The row consists of 6 main structures with support bars, upper and lower foundations, girders with horizontal crossbeams and a pressure bar connecting the upper and lower foundations (see Figure 1a). The 6 main structures are connected with 5 intermediate structures. The row has a net height of 3.5 m, defined as the average distance of the upper edge of the supporting surface from the ground normal to the line of slope. The site was chosen because of its good accessibility, the high snow depths in recent winters, which are mainly due to heavy accumulation of drift snow, and most importantly because of the high snow pressure forces measured in previous measurement campaigns (Hiller and Bader, 1990).
A total of six measuring points were chosen at various support and pressure bars of the supporting structure. Each measuring point consists of a strain gauge (HBK 1XY11-3/350), a temperature sensor (PT1000) and an amplifier (FGCDMSv2), all of which are protected from moisture, dirt and dust by a sealed box. The strain gauges are glued to the steel with two-component adhesive (X60) after the surface has been derusted and smoothed. The strain gauge and the temperature sensor are connected to an amplifier that converts the analogue signal into a digital signal. The sealing box, which is equipped with a waterproof RJ45 interface, is attached to the steel with silicone and two-component adhesive. We used adhesives to increase friction instead of fastening systems that increase normal pressure (e.g. steel straps, screws) to avoid localised stress concentrations that affect the strain measurement. The digital signal from the amplifiers is transmitted to the main board (FGCMBV2) via RJ45 cables inside the horizontal crossbeams to protect the cables from UV radiation and snow settlement forces. The energy supply is guaranteed by a 175 W solar panel in combination with a 1080 Wh battery. The measurement interval is 5 min to ensure a sufficient temporal resolution to capture the daily cycle of forces. The measured data is transmitted once a day via mobile connection.

2.1 Calculation of strains, stresses and forces

The supply voltage V_s of the strain gauges is 10 V. The strain given a certain differential voltage at the input of the measuring amplifier is then

$$\epsilon = \frac{V_0}{1+\nu}\frac{4}{kV_s} \tag{1}$$

where ν is Poisson's ratio (0.3 for steel), k is a characteristic coefficient of the strain gauge (2.05 according to data sheet) and V_0 is the measured voltage difference. As an example, with a longitudinal strain of 10 μm/m, we expect a differential voltage of 0.066625 mV at the input of the amplifier. The strain can then be used to calculate the normal force in the support or pressure bar using Hooke's law

$$F = \epsilon EA \tag{2}$$

The resulting snow pressure force along the girder can then be reconstructed using the static system of the supporting structure. The instrumented support and compression bars have freely rotating hinges at both ends so that they can be regarded as simple tension and compression bars if the settlement pressure due to the snow behind the steel bridge is neglected. The upper foundation can only take up normal loads from tension and no shear forces. Therefore, the static system of this pressure bar type of construction is determinate, which facilitates the calculation of the normal forces from the external loads considerably (Margreth et al., 2014). Figure 2 shows that if the steel bridge is completely buried in the snow and the snow pressure is assumed to be uniformly distributed over the snow depth, a unit load of 1 kN along the girder leads to a normal force in the supporting and compression bars of approximately -0.5 kN or -0.35 kN respectively.

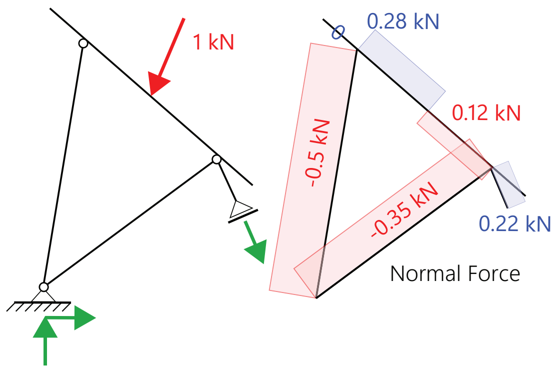

Figure 2: Left: Static system of the supporting structure (Margreth et al., 2014) with resultant unit snow pressure (red) and reaction forces (green). Right: resulting normal forces from unit load.

2.2 Compensation of temperature-induced strains

A non-supported steel bar undergoes temperature-induced strains of approximately 12 $\frac{\mu m}{m\,^{\circ}C}$. At expected average snow pressure induced strains of 100 $\frac{\mu m}{m}$, temperate-induced strains have a strong influence on the measurements and cannot be neglected. We used a number of countermeasures to make sure that only strains caused by snow pressure are taken into account. Firstly, the strain gauges used are bidirectional and measure the strain in the longitudinal and transverse direction of the bar (see Figure 1c). Assuming that the temperature-induced strain is isotropic and the stresses induced by the snow in the transverse direction are negligible, the temperature-induced strain in the longitudinal direction can largely be filtered out with this setup. A preliminary test showed that this reduces temperature-induced strain to approximately 0.5 $\frac{\mu m}{m\,^{\circ}C}$. Secondly, a supporting structure is selected, which is usually completely buried in the snow. As the highest temperature differences are reached when the support bars are exposed to direct sunlight, temperature-induced strain is drastically reduced if all the support bars are completely below the snow surface. In addition, one measurement point was placed on a free end of the tension bar connected to the upper foundation. This free end is not loaded and therefore only has temperature-induced strain. This control measurement can therefore be used to quantify this temperature effect. Finally, the temperature of all strain gauges is measured simultaneously with the strain. This data can be used in combination with the control measurement to recognise patterns between temperature and strain, which can be corrected retrospectively.

3. RESULTS

The winter of 2023/24 in Switzerland was characterised by large differences in snow depth depending on altitude. Above 2000 metres above sea level, which also applies to the instrumented location, the snow depths were above the long-term average throughout the winter. The 45 automatic stations in this altitude zone, which have been in operation since at least 1999, show an average relative snow depth of 123% over the period from November to March, which corresponds to fifth place in the last 25 years (Zweifel, 2024). Figure 3 shows the development of forces in the supporting structure as well as the snow height, surface and air temperature of the nearest IMIS meteo station (500 m distance). In February and March, the measured forces in the support and pressure bar continuously increased. This period was characterised by low temperatures with regular snowfall events. The period from 15-18 February was an exception. During this period, there was no cloud cover with warm temperatures (between 1°C and 5°C) during the day and cold temperatures (between -10°C and -5°C) at night. This led to a characteristic daily cycle of the forces, with the local maximum being reached at sunrise, followed by a sharp decrease during the day until sunset. After sunset, the forces slowly increase again until the next sunrise. In the period from 6-16 April, there was a prolonged period of foehn winds. This phenomenon led to high temperatures above freezing temperature even during the night and thus to a drastic reduction in snow depths (from 260 cm down to 220 cm) and forces. On some nights the sky was cloudless, which led to surface temperatures well below zero and thus again to the characteristic increase in forces during the night with the local peak at sunrise. The warm period was followed by very low temperatures from 17 to 29 April with a daily

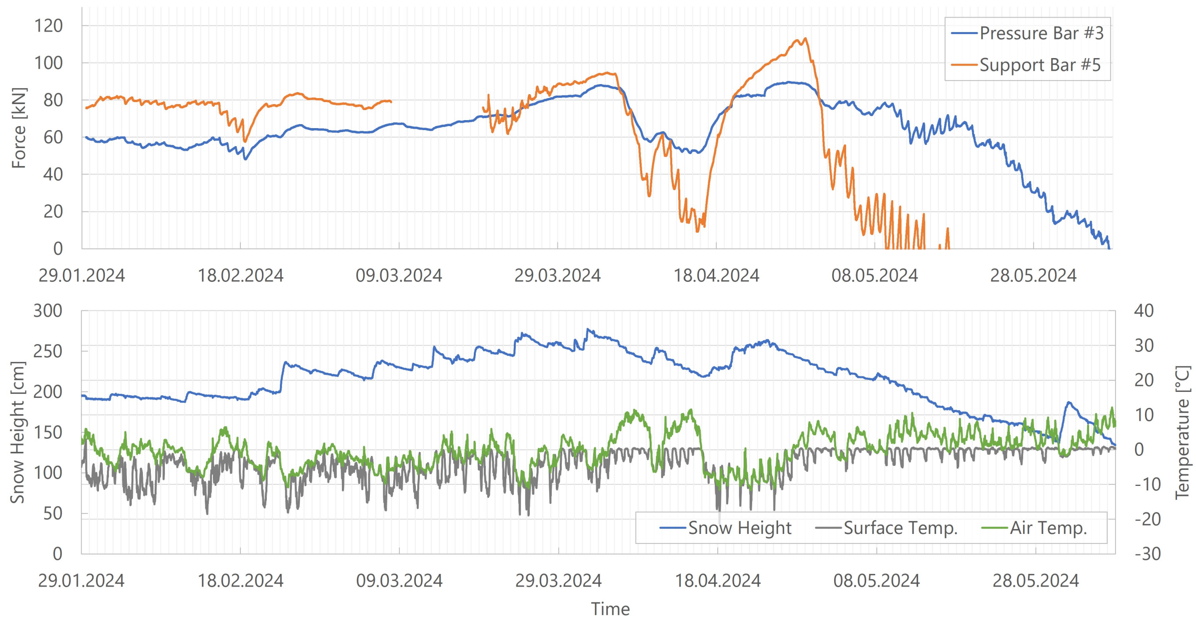

Figure 3: Forces over time in support and pressure bar calculated from the measured strain (top). Positive forces represent pressure forces. IMIS meteodata from the nearby station "Kreuzweg" (bottom). Each vertical grid line represents midnight.

mean air temperature of -10°C, which led to a strong increase in forces without a daily cycle pattern. The annual maximum force of 110 kN in the support bar and 90 kN in the compression bar is reached on 29 April at sunrise. Using the static system (see figure 2), this corresponds to a resultant force along the girder of approximately 220 kN or 88 kN/m' for a field width of 2.5m. After reaching the maximum, the forces decrease again in May, as the air temperatures are constantly high and there are no more major snowfalls. Similar to the foehn period, there were some clear nights in which the snow surface temperature dropped well below zero and the forces in the beams recovered temporarily. The force in the support bar reaches zero at a snow depth of 180 cm. The force in the pressure bar reaches zero at a snow depth of 125 cm.

4. DISCUSSION

The measurements during the winter of 2023/2024 showed consistent correlations between temperature and forces. Firstly, during warm periods (air temperature $\gg$ 0, snow surface temperature = 0) the forces decrease continuously, seemingly without a time limit. Secondly, if a warm period is followed by a cold period, the forces increase. This increase in forces is limited and only lasts until the point at which all the wet snow is frozen again. If the temperatures are low over a long period of time, the forces remain constant apart from the additional mass caused by snowfall events. Since the snow cover melts and freezes from the snow surface in a downward direction, these decreases and increases in force are much more pronounced in the support bar. This temperature dependence and the resulting diurnal variation of the forces was also observed in the load cell measurements of Hiller and Bader (1990) and Larsen et al. (1985), although it was never possible to fully explain the reasons for this phenomenon, mainly because the behaviour is counterintuitive. At high temperatures, high forces are to be expected due to severe sliding of the snow at the base. Larsen et al. (1985) even debated whether this behaviour is really caused by the snow pressure or rather by the freezing and thawing of the load cells. In the current setup, however, freezing and thawing cannot be an issue as there are no moving parts in the sensor. Measurements on snow nets also showed similar behaviour with the suspicion that the steel warms up in sunlight, melting the connecting snow layer so that the snow cover is temporarily not retained by the net and the forces therefore decrease (Margreth, 1995). One argument against this theory is that in this case, the steel bridge was completely buried in snow and was never exposed to direct sunlight until the beginning of June.

One explanation for this temperature dependency is that when the wet snow freezes, the internal stresses can be transferred much better in a horizontal direction and thus the influence zone of the snow on the support structure increases. This is comparable to the earth pressure coefficient in soil mechanics: when the snow is wet, the stresses in the snow cover can only be transferred poorly in a horizontal direction, the earth pressure coefficient is small and most of the force is transferred into the soil due to gravity. If the wet snow freezes, the horizontal force transfer is much greater, which means a higher earth pressure coefficient and the forces are increasingly transferred not only into the ground but also horizontally (or parallel to the slope) into the support structure. In the case of slender obstacles such as the supports of photovoltaic systems, this effect is likely to be even stronger, because in addition to the force transfer parallel to the slope, the force transfer in the direction transverse to the slope is of additional importance.

The force in the support bar reaches zero before the force in the pressure bar. This makes sense, because when the snow depth falls below the height of the girder, more and more force is channelled into the upper foundation and the pressure bar instead of the support bar. Load case 1 (fully buried structure) turns into load case 2 (partially buried structure), which influences the load distribution in support and pressure bars Margreth (2007). In extreme cases of load case 2, even tension forces may occur in the support bar. The reason why the forces in the pressure bar also reach zero long before the snow is gone is because the supporting structure heats up at low snow depths and melts all the surrounding snow connected to it.

Although Hiller and Bader (1990) instrumented the same steel bridge presented in this paper, comparisons are difficult due to the strong influence of temperatures and climatic conditions on the snowpack and the associated snow depth, density and sliding properties. In the 20 years of measurements, there were winters with little snow and thus maximum forces of only 5 kN/m. The highest force of this earlier measurement series was 46 kN/m, measured in the avalanche winter of 1998/1999. Although the snow depth in winter 2023/2024 was also above average, the measured forces are clearly too high. One possible reason for these too high forces is the additional static and settlement force caused by the fact that the support and pressure bars are completely buried in the snow. This additional load causes bending and an additional normal force due to friction, both of which lead to an increase in the measured (compressive) strain. One indication that this force may not be negligible is that the sensor box on the support bar was sheared off in early March and had to be replaced. Another reason for the excessive forces is that the sensors showed a strong drift as soon as the forces became small. As strain measurements are always relative and the measurement series could only be started in the middle of winter, it was difficult to retrieve the zero value of the strain in spring in order to convert the relative strains into absolute values. This problem is to be solved next winter when the entire season can be measured.

4.1 Temperature-induced Strain

Figure 3 confirms that the proposed setup successfully filters out temperature-induced strains. However, the fact that the steel bridge was completely buried under snow for most of the winter and thus kept temperature variations to a minimum was helpful. At the beginning of March, the sensor on support bar 5 had to be replaced. After the sensor was back in operation on 19 March, the support beam was still free of snow until it was completely covered again on 28 March. During this time, some temperature effects are visible in the results, but they only vary in the range of $\pm$ 3 kN. One of the reasons why temperature-induced strains cannot be compensated completely is that analogue electronics also has a temperature dependency.

4.2 Installation Improvements

Several improvements are planned for next winter. Firstly, the support and pressure bars need to be instrumented with two bi-axial strain gauges on both sides. With this setup, the strain due to bending can be separated from the strain due to normal force in order to better filter out the effects of settlement pressure. Additionally, simple maximum force indicators (e.g., Brinell hardness test) are installed as a plausibility test. The sensor boxes, even if they are located on the back of the steel bridge, must be protected from settlement pressure. The same applies to the cables. It is not enough to protect them inside the horizontal crossbeam from pressure from above (see Figure 1a and d), because when wet snow freezes around the cables, it pulls the cables down as the snow settles underneath. Ideally, the cables should be buried or run in thin steel pipes whenever possible to avoid problems. In addition, the cables must be protected from rodents in summer if the installation is planned for several years. Finally, an extensive field campaign is planned for the upcoming winter, where local snow distribution, snow temperature and density is regularly measured. Despite the problems encountered during the first winter, the system is a promising first step towards a low-cost, non-invasive monitoring solution that is crucial for future research into the design of structures exposed to snow pressure.

ACKNOWLEDGEMENT

We thank Davos Klosters Bergbahnen AG for allowing us to instrument their supporting structures, which was crucial for obtaining the data presented in this paper.

References

Bader, H., Haefeli, R., Bucher, E., Neher, J., Eckel, O., C.Thams, and Niggli, P.: Der Schnee und seine Metamorphose, Beiträge zur Geologie der Schweiz. Geotechnische Serie. Hydrologie, Lieferung 3, 1939.

Fellin, W.: Einführung in Eis-, Schnee- und Lawinenmechanik, Springer Berlin Heidelberg, doi:10.1007/978-3-642-25962-3, 2013.

Haefeli, R.: Schneemechanik mit Hinweisen auf die Erdbaumechanik, Ph.D. thesis, ETH Zurich, doi:10.3929/ethz-a-000096665, 1939.

Hiller, M. and Bader, H.: Schneedruck auf Stützwerke, Tech. rep., WSL Institute for Snow and Avalanche Research SLF, Interner Bericht Nr. 660, 1990.

Larsen, J. O., McClung, D. M., and Hansen, S. B.: The temporal and spatial variation of snow pressure on structures, Canadian Geotechnical Journal, 22, 166–171, doi:10.1139/t85-023, 1985.

Margreth, S.: Snow pressure measurements on snow net systems, in: Proceedings of the ANENA Symposium May 30-June 03, pp. 241–248, 1995.

Margreth, S.: Defense structures in avalanche starting zones, Tech. rep., Federal Office for the Environment, Bern and WSL Institute for Snow and Avalanche Research SLF, Davos, technical guideline as an aid to enforcement, 2007.

Margreth, S., Suda, J., Mölk, M., Hofmann, R., Gauer, P., Schilcher, W., Skolaut, C., Mears, A., and Sauermoser, S.: Structural avalanche defense: design and construction, chap. 6, pp. 177–254, John Wiley & Sons, Ltd, doi:10.1002/9783433603840.ch06, 2014.

Podolskiy, E., Chambon, G., Naaim, M., and Gaume, J.: A review of finite-element modelling in snow mechanics, Journal of Glaciology, 59, 1189–1201, doi:10.3189/2013JoG13J121, 2013.

Salm, B.: Snow Forces, Journal of Glaciology, 19, 67–100, doi:10.3189/S0022143000029221, 1977.

SLF: Der Lawinenwinter 1999, Tech. rep., WSL Institute of Snow and Avalanche Research SLF, 2000.

Zweifel, B.: SLF Winterflash 2023/24, URL https://www.slf.ch/de/lawinenbulletin-und-schneesituation/winterberichte/winterbericht-202324, 2024.